Dynamics of Rotors on Hydrodynamic Bearings

R. Eling[*1], R. van Ostayen[2], D. Rixen[3]
[1]Mitsubishi Turbocharger and Engine Europe, [2]Delft University of Technology, [3] Technical University Munich
*Corresponding author: reling@mtee.eu

Abstract: Rotordynamic analysis is a crucial step in the development of rotor bearing systems in order to prevent rotor instabilities, excessive unbalance response, bearing overheating or other undesired phenomena.
This study presents a rotordynamic analysis of a rotor supported by hydrodynamic bearings using Comsol Multiphysics. In this paper, the complexity of the model is gradually increased. Starting point of the analysis is the modal analysis of the rotor in free-free conditions, as it can be accurately validated by experiments. Once the rotor modal properties correspond with experimental values, the hydrodynamic bearing properties are investigated. A Reynolds model is set up to predict the lubricating film pressure distribution under shaft loading. Due to the cross coupling terms of the bearing stiffness coefficients, instability may occur. A point mass simulation of the shaft in a hydrodynamic bearing is able to predict the whirl frequency and amplitude of the bearing itself. Coupling the hydrodynamic bearings to a flexible shaft, the whirl can be seen to interact with the rotor natural frequencies.
Hence, by coupling the fluid film physics directly to the rotor physics, a prediction of the rotor dynamics can be made. This enables the design engineer to evaluate the critical rotor bearing design criteria at a very early stage of development.

Keywords:
Rotordynamics, fluid film, hydrodynamic bearings, unbalance response, whirling, Campbell diagram, turbocharger

1. Introduction

Fluid film bearings are used in a wide variety of high speed, high load and high precision applications due to their excellent lifetime performance, low cost and low noise output. A hydrodynamic bearing consists of a thin layer of fluid which separates two objects which have a relative motion. The working principle is based on the hydrodynamic pressure generation in the fluid: when shear flow forces the fluid into a converging section, an increase of pressure will occur, see Figure 1. The increase of pressure counteracts the rotor load and hence the film has a certain carrying capacity.

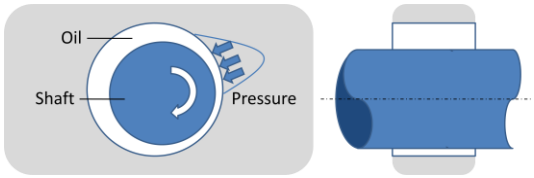

Figure 1 Working principle of a hydrodynamic bearing. The shaft rotation generates a shear flow of oil. The resulting pressure distribution interacts with the shaft loads.

The fluid films support the rotor loads in radial and axial directions. The load carrying capacity of the fluid film is created by the shaft movement itself. Therefore, a coupled analysis of the rotor structure and the fluid domain is necessary to obtain realistic predictions of the operational response over the entire rotor speed range.

In this paper, the analysis steps taken to evaluate the design of a rotor bearing system are illustrated. The analysis starts by analyzing the uncoupled rotor structure. This is followed by an analysis of the uncoupled bearing. After the rotor and bearing properties have been illustrated, the interaction between the rotor and the bearing dynamics is investigated in a coupled analysis.

This kind of study can typically be made at a very early stage of developing a new rotor bearing system. As a result, the correct geometry can be configured at the very first prototype phase and undesired rotor responses can be prevented.

Hydrodynamic bearings are applied to support rotors in a wide range of rotating machinery, varying from MEMS rotors to hydro turbines with power levels of over 100MW. In this study, the focus will be on a turbocharger rotor for automotive applications.

2. Turbocharger rotor bearing system

The system under consideration is an automotive turbocharger rotor bearing system. It features two overhung wheels on a steel shaft, suspended on oil lubricated hydrodynamic bearings, both in radial and in axial directions. For this analysis, we will focus only on the radial dynamics; the axial dynamics are relatively straightforward and are ignored here. The turbine wheel is connected to the shaft by a weld whereas the compressor wheel is assembled by a simple nut connection in axial direction.

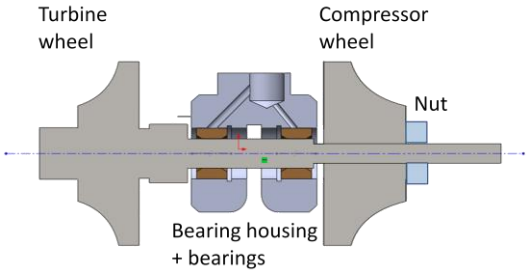

Figure 2 Schematic cross section of a turbocharger rotor bearing system.

The operation speed of an automotive turbocharger is varying constantly, and can be over 250.000rpm for small size turbochargers. At these speeds, the rotating unbalance excitation frequency is above the first rotor bending eigenfrequency and therefore the rotor can no longer be considered to be rigid. Instead the rotor behaves as a flexible shaft, and therefore has to be modeled with sufficient degrees of freedom to capture the different flexible shaft modes.

For the development of a turbocharger rotor bearing system, multiple performance criteria have to be evaluated [2]:

- **Stability** of the rotor to ensure safe operation under all operating conditions, including variable oil supply temperatures, variable rotation speeds and various unbalance loading configurations.
- Rotor **response to unbalance** to prevent wear and noise issues. In addition, minimization of the shaft orbit allows for reduction of the required rotor-stator gap. This results in less air flow leakage and thus better turbine and compressor efficiencies.
- **Friction losses** in the bearings to improve the overall turbocharger efficiency and to reduce spin-up times.
- Perhaps most importantly, **the production cost** of the total rotor bearing system has to be minimized for the competitive automotive market.

In order to meet these often conflicting requirements, a structured approach is required.

When designing a rotor bearing system, a typical rotor dynamic analysis consists of the following steps [3]:

1. Modal analysis of the stationary rotor
2. Determination of the rotor eigenfrequencies as a function of rotation speed, resulting in the Campbell diagram
3. Prediction of the unbalance response of the linear system
4. Calculation of the bearing stiffness and damping coefficients
5. Stability analysis and run-up simulation of the coupled system

The complexity of this analysis strongly depends on the bearing coefficients: linear, symmetric bearings allow relatively straightforward methods whereas non-linear and asymmetric bearing coefficients require more elaborate analysis. The turbocharger rotor bearing system under consideration has highly non-linear and asymmetric bearing coefficients. In the following sections, the analysis will start using a simple linear rotor model and will gradually be developed into a coupled rotor-bearing model.

3. Modal analysis of the stationary rotor

Typically, the first step in modeling the dynamics of a rotor bearing system is the modal analysis of the stationary rotor. This means that the influence of the bearings is excluded first. The rotor geometry is discretized using finite elements. Modal analysis is performed to obtain the eigenfrequencies and the associated eigenmodes of the rotor in free-free conditions. The simulation results from the modal analysis can easily be validated using impact hammer testing, followed by a modal assurance criterion study between experimental and simulation results. In this case, the range of interest is 0-

6kHz in which two bending modes are found, see Figure 3. The range of interest is based on the first order (unbalance) excitation of the rotor.

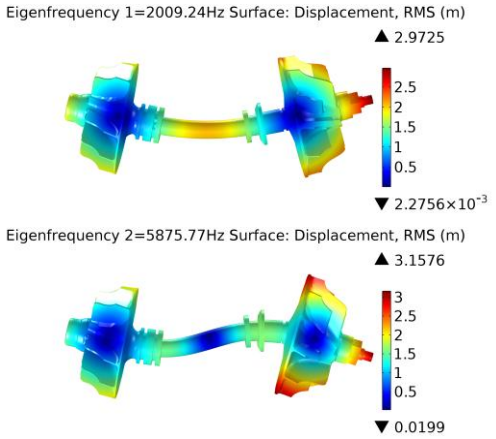

Figure 3 Mode shapes belonging to the first two eigenfrequencies of the rotor in free-free conditions.

The 3d finite element model can be used to perform detailed geometry analysis, such as investigating the effect of contact stiffness between the individual rotor elements and determining the effect of local pre-stress due to the nut fastener assembly. In the case of our turbocharger rotor bearing system, the assumption of rigid contact is made and pre-stress from the specified compressor nut torque is added. This results in eigenfrequency predictions within 2% of the experimental modal analysis results.

The downside of using a 3d finite element model which is based on volume elements is the large number of nodes. This requires a lot of computation power, especially in time transient analysis which will be performed by the coupled model. As the rotor essentially has a simple and axisymmetric design, the volume elements can be replaced by simple beam and disk elements as depicted in Figure 4. For comparison: the full finite element model uses 75.000 volume elements whereas the beam model only uses 10 simple beam elements.

Special attention has to be given to the shaft-disk interface. In practice, the disk elements are often bolted, shrunk-fit or welded to the shaft and hence the disks add stiffness and mass to the shaft.

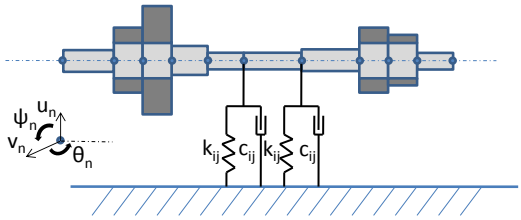

Figure 4 Beam and disk element model of a turbocharger rotor bearing system, where i,j={X,Y}

Different approaches can be chosen to include these added mass and stiffness properties [1,3]. Depending on the approach, the beam-disk finite element model can be updated using either the full finite element model results or the experimental results.

4. Critical rotation speeds

The next step in the analysis is to evaluate the rotordynamics of the rotor-bearing system over the entire speed range. For this step, the previously described beam-disk element model is complemented with bearing, see Figure 4. For this step, initially the most basic bearing representation as linear and symmetric springs and dampers is used. The equations of motion of this system are:

$$\mathbf{M}\ddot{\mathbf{q}} + (\mathbf{C} + \Omega\mathbf{G})\dot{\mathbf{q}} + \mathbf{K}\mathbf{q} = \mathbf{F}$$

$$with\ \mathbf{q} = [u\ v\ \theta\ \psi]^T$$

where **M**, **C**, and **K** denote the mass, damping and stiffness matrices respectively, **F** denotes the force vector describing the aero and unbalance load, Ω is the rotation speed and **G** is the gyroscopic matrix of the beam and disk elements. Due to the gyropscopic effect, the eigenfrequencies of the system become a function of rotation speed. The complex conjugate roots of the characteristic equation split up into one forward whirling mode and one backward whirling mode, as can be seen in the Campbell plot, see Figure 5. In this case the undamped eigenfrequencies are plotted, where the damping **C** is assumed to be zero.

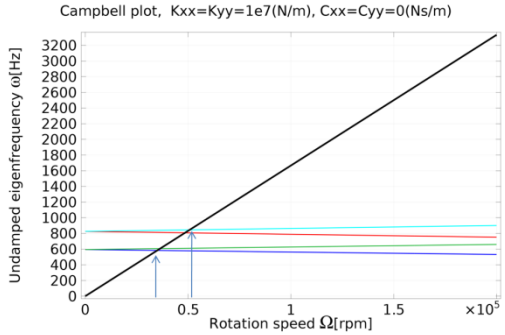

Figure 5 Campbell plot showing the undamped eigenfrequencies as a function of rotation speed of the rotor on linear stiffness bearings without damping.

In the Campbell plot, the modes which have an increasing eigenfrequency are the forward whirling modes. Critical speeds are speeds where the rotation frequency is equal to an eigenfrequency. Under symmetric bearing supports, only the forward whirling modes are excited by unbalance excitation [3]. Hence, an increase of vibration is to be expected at rotation speeds (or near rotation speeds, in case damping is added) of 36.000rpm and 51.000rpm.

5. Unbalance response using linearized bearing coefficients

Having found the critical speeds, the potentially dangerous rotation speeds are found. In case there is an amount of unbalance on the rotating structure, it causes a harmonic excitation. Figure 6 gives the rotor displacement response to an unbalance located on both wheels. In this case, the unbalance vectors were modeled to be in phase with each other. Indeed, the critical speeds at 36.000rpm and 51.000rpm give an increased response. The maximum tip displacement is a critical value as the stator gap needs to be small in order to minimize leakage flow in the turbine and compressor. In the same manner, other critical aspects such as maximum shaft stresses and bearing reaction forces can conveniently be evaluated over the entire speed range of the rotor.
Note that for demonstration purposes, only a small amount of damping was added here. Hydrodynamic bearings usually have high damping coefficients.

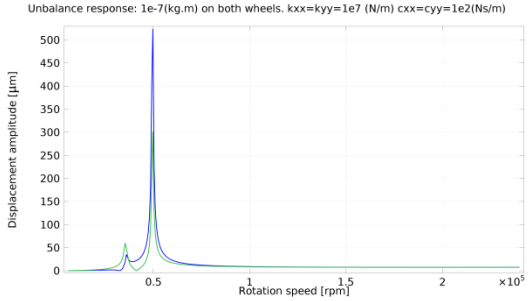

Figure 6 Unbalance response of rotor displacement evaluated on the wheel locations using linear bearing coefficients revealing two critical speeds. The second whirling mode near 51.000rpm is clearly the most sensitive mode.

6. Calculation of the bearing stiffness and damping coefficients

In the previous analyses, linear bearing coefficients were assumed for demonstration purposes. Hydrodynamic bearings however, generally have non-linear and rotation speed dependent stiffness and damping properties.

The stiffness and damping properties of a hydrodynamic bearing originate from shear flow and squeeze motion, see Figure 1. Hence, the pressure distribution in the fluid film needs to be calculated as a function of rotation speed and rotor position. Owing to the thin film height, the Reynolds equation can be used to describe the fluid flow. As the film curvature is small compared to the axial and circumferential lengths, an *unfolded* bearing model can be assumed, using Cartesian coordinates *(x,y,z)* for circumferential, radial and axial directions, the Reynolds equation is written as [5]:

$$\frac{\partial}{\partial t}(\rho h)+\frac{\partial}{\partial x}\left(\frac{\rho h}{2}U\right)=\frac{\partial}{\partial x}\left(\frac{\rho h^3}{12\mu}\frac{\partial P}{\partial x}\right)+\frac{\partial}{\partial z}\left(\frac{\rho h^3}{12\mu}\frac{\partial P}{\partial z}\right)$$

where U denotes the wall velocity of the rotating surface, ρ is the (constant) fluid density, μ is the (constant) fluid viscosity and P is the pressure. The variable h is the film height function, which depends on the rotor position. In case the bearing axial length L is either much shorter or much longer than the bearing diameter D, analytical solutions for the Reynolds bearing equation exist.

In the case that $L/D \approx 1$, as for a turbocharger bearing, a numerical approximation for the

pressure distribution has to be made, based on finite element discretization in 2d. The resulting pressure distribution in such a journal bearing can be seen in Figure 7. The results were compared with analytical solutions [5] assuming either $L/D \gg 1$ or $L/D \ll 1$ where the Reynolds equation is only solved in one direction.
The results show that in case $L/D \approx 1$, significant differences are found between the analytical and the numerical results, especially at large eccentricities. Therefore, in case $L/D \approx 1$, the 2d Reynolds model has to be used.

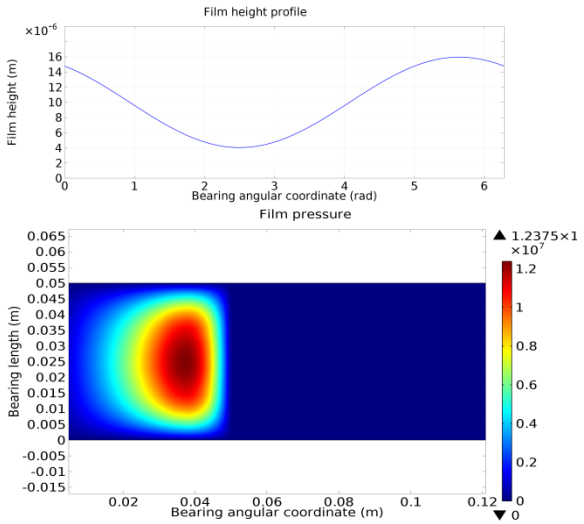

Figure 7 Bearing film height function and the resulting pressure distribution evaluated at a shaft eccentricity of 0.5 times the total bearing clearance

The increase of pressure as depicted in Figure 7 comes from the convective acceleration at the converging section of the fluid domain. At the diverging section, the standard Reynolds solution would predict negative fluid pressures. In reality, cavitation occurs in this section. A mass-conserving cavitation model [6] as an extension to the Reynolds equation is used to accurately predict the fluid cavitation and reformation zones. This way, a more realistic (non-negative) pressure distribution is calculated.

In addition, the pressure distribution is strongly influenced by the fluid viscosity. Shear flow in viscous fluids generates heat and therefore the fluid viscosity is a function of the rotation speed and rotor load. The mass conserving cavitation algorithm enables a more realistic energy balance prediction, because the difference of shear flow losses and heat transfer coefficients between fluid and gas phases can be taken into account.
To obtain the bearing stiffness and damping coefficients, small perturbations of displacement and velocity around an equilibrium rotor position are applied:

$$K_{a,b}\Big|_{\varphi_{eq},\varepsilon_{eq}} = \frac{\partial F_a}{\partial b}\Big|_{\varphi_{eq},\varepsilon_{eq}} \qquad C_{a,b}\Big|_{\varphi_{eq},\varepsilon_{eq}} = \frac{\partial F_a}{\partial \dot{b}}\Big|_{\varphi_{eq},\varepsilon_{eq}}$$

$$with\{a,b\} = X,Y$$

where the forces F_X and F_Y are found by integrating the pressure distribution over the bearing area. These stiffness and damping terms can be calculated either by numerical perturbation or analytically using the 1d Reynolds descriptions. As the 2d Reynolds description is more suitable here, numerical perturbation is used.

As an example, Figure 8 gives the resulting bearing stiffness coefficients as a function of the shaft eccentricity, evaluated at a rotation speed of 100.000 rpm. Although not depicted here, the stiffness and damping coefficients obviously depend on the rotation speed as well. The model used in this case considers one single lubricating fluid film. In practice many turbocharger manufacturers use so-called floating ring bearings which basically consist of two of these films in series [2].

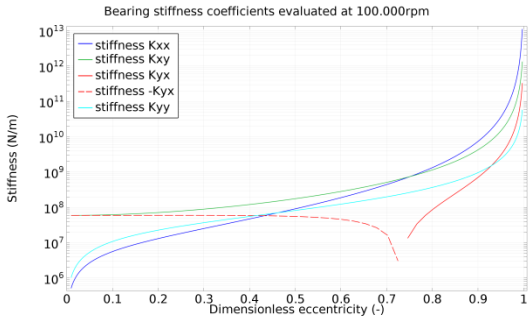

Figure 8 Bearing stiffness evaluated at 100.000rpm

At low to medium shaft eccentricity, the cross coupling stiffness terms dominate. The stiffness term K_{YX} even shows negative stiffness. These two properties are typical for such a hydrodynamic bearing, and can be understood by considering Figure 7: the resultant force from the

fluid pressure has some phase lag relative to the angular position of maximum deflection.

As K_{XX} is not equal to K_{YY}, unbalance loads on hydrodynamic bearings can excite both the forward as well as the backward whirl modes of the rotor[4].
The large (and negative) cross coupling terms cause bearing instabilities [2,3,5]. Performing a simple Routh-Hurwitz stability analysis on a linearized point mass 2 degrees of freedom system shows:

$$\chi_{stable} = \frac{-K_{XY}K_{YX}}{K_{XX}K_{YY}} \leq \chi_{unstable}$$

This reveals that the system is linearly unstable, but can be stabilized by decreasing the ratio of cross-coupling stiffness versus direct stiffness of the bearing.

7. Non-linear analysis: evaluating bearing stability using a rigid rotor

The Routh-Hurwitz criterion is an interesting preliminary analysis for the stability of the rotor-bearing interaction, but it does not take into account the strong non-linearity of the bearing coefficients as can be seen in Figure 8. In order to include the non-linear bearing behavior, the thin film bearing model is loaded harmonically with a rotating unbalance in a time transient analysis, using the following equations of motion:

$$\mathbf{M}\ddot{\mathbf{e}} = \mathbf{F}_{fluid} + \mathbf{W}_{unb}$$

$$with\, \mathbf{e} = [X, Y]^T$$

In this analysis, the unbalance forces W_{unb} are harmonic and the fluid film forces F_{fluid} are found by integrating the thin film pressure solution over the bearing area.

Under light unbalance loads, bearing limit cycle stability is observed. The shaft is unable to find a stationary equilibrium position, but instead will start to whirl as can be seen in Figure 9. The orbit is the superposition of two types of whirl. The whirl coming from unbalance excitation has a frequency equal to the rotation speed and is called the synchronous whirl. The bearing instability usually has a frequency close to Ω/2 and is therefore called sub-synchronous whirling.

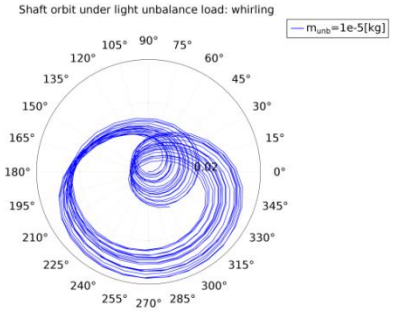

Figure 9 Whirling of a rigid rotor supported on a hydrodynamic bearing showing a superposition of synchronous and sub-synchronous whirl.

Whirling motion means that an amount of energy will be dissipated by the bearing, which can be undesirable for shaft fatigue and noise. More importantly, when the bearing whirling frequency coincides with one of the rotor natural frequencies, a resonance called *oil whip* occurs which can even lead to complete rotor failures [3].

8. Non-linear analysis: response of a flexible shaft on hydrodynamic bearings

The final step of this study is to couple the flexible shaft to two individual hydrodynamic bearings. In Comsol, the fluid films are analyzed using the Thin Film Module. The rotor model can either be generated using the Beam Module or can be written as a finite element description [3] in the ODE module.
The resulting rotor response is analyzed by performing a time-transient analysis over several rotations. Transforming the time-transient signal to the frequency domain reveals the response of the synchronous and the sub-synchronous whirl, see figure 10.

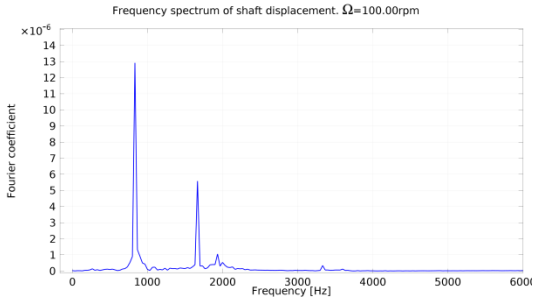

Figure 10 Frequency spectrum of the coupled rotor-bearing displacement response showing both

synchronous (1667Hz) as well as sub-synchronous vibration.

When the rotor response over the full operation range needs to be evaluated, a parameter sweep can be used. This represents a quasi-steady acceleration which can be allowed in case of a turbocharger: the change of rotation speed over several rotations is nearly zero.

Figure 11 gives an example of such a response curve: the RMS values of shaft displacement are evaluated over the rpm range. This plot shows how the compressor wheel passes through a mild critical speed near 80.000rpm. The sudden increase of the vibration level of the bearing node near 120.000rpm indicates that a strong whirling mode occurs in the bearings. Also the response of the compressor wheel increases strongly after 120.000rpm, indicating an increased sensitivity to unbalance in the coupled rotor bearing system at speeds above 120.000rpm. By carefully selecting the rotor bearing design, such sensitivities can be decreased. Hence, issues with rotor failure, bearing wear or excessive noise can be avoided.

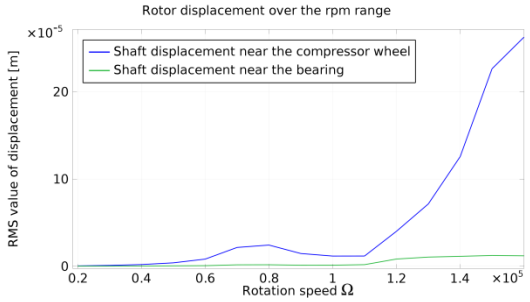

Figure 11 Response to unbalance of the coupled rotor bearing system

9. Conclusions

Modeling the rotor dynamics of rotors on hydrodynamic bearing requires several steps to understand and explain the complex rotor behavior over the operation range. As the hydrodynamic bearing contains cross coupling stiffness terms, instabilities of the coupled system can result in excessive rotor vibration values. The results of adjustments in the rotor bearing design can now be evaluated on the most important performance criteria.

Further analysis will be focused on applying the developed methods to analyze more complex hydrodynamic bearings such as the floating ring bearing. The final aim is to build a fully parametric Comsol model which can be used for robust optimization of a turbocharger rotor bearing system.

8. References

[1] Hemberger, D. Filsinger, D. and Bauer, H., Mistuning modeling and its validation for small turbine wheels, Proceedings of the ASME Turbo Expo, GT2013-94019, (2013)

[2] Nguyen-Schäfer, H., *Rotordynamics of Automotive Turbochargers*, Springer-Verlag, Berlin Heidelberg (2012)

[3] Friswell, M., Penny J., Garvey, S and Lees, A., *Dynamics of rotating machinery*, Cambridge University press, New York (2010)

[4] Greenhill, L. and Cornejo G., *Critical speeds resulting from unbalance excitation of backward whirl modes*, Design engineering technical conferences, Volume 3 part 3-B, ASME (1995)

[5] San Andrés, L., *Lecture notes Modern Lubrication Theory*, Texas A&M Rotordynamics laboratory (2012)

[6] Van Ostayen, R., Van Beek, A. *Thermal modelling of the lemon-bore hydrodynamic bearing*, Tribology International Vol. 42 issue 1, Elsevier (2009)